A&A 518, L31 (2010)
DOI: 10.1051/0004-6361/201014552

Herschel: the first science highlights

Astronomy & Astrophysics
Special feature

Letter to the Editor

The far-infrared/radio correlation as probed by *Herschel*★

R. J. Ivison[1,2], B. Magnelli[3], E. Ibar[1], P. Andreani[4,5], D. Elbaz[6], B. Altieri[7], A. Amblard[8], V. Arumugam[2], R. Auld[9], H. Aussel[6], T. Babbedge[10], S. Berta[3], A. Blain[11], J. Bock[11,12], A. Bongiovanni[13], A. Boselli[14], V. Buat[14], D. Burgarella[14], N. Castro-Rodríguez[13], A. Cava[13], J. Cepa[13], P. Chanial[10], A. Cimatti[15], M. Cirasuolo[1], D. L. Clements[10], A. Conley[16], L. Conversi[7], A. Cooray[8,11], E. Daddi[6], H. Dominguez[17], C. D. Dowell[11,12], E. Dwek[18], S. Eales[9], D. Farrah[19], N. Förster Schreiber[3], M. Fox[10], A. Franceschini[20], W. Gear[9], R. Genzel[3], J. Glenn[16], M. Griffin[9], C. Gruppioni[21], M. Halpern[22], E. Hatziminaoglou[4], K. Isaak[9], G. Lagache[23], L. Levenson[11,12], N. Lu[11,24], D. Lutz[3], S. Madden[6], B. Maffei[25], G. Magdis[6], G. Mainetti[20], R. Maiolino[17], L. Marchetti[20], G. E. Morrison[26,27], A. M. J. Mortier[10], H. T. Nguyen[11,12], R. Nordon[3], B. O'Halloran[10], S. J. Oliver[19], A. Omont[28], F. N. Owen[29], M. J. Page[30], P. Panuzzo[6], A. Papageorgiou[9], C. P. Pearson[31,32], I. Pérez-Fournon[13], A. M. Pérez García[13], A. Poglitsch[3], M. Pohlen[9], P. Popesso[3], F. Pozzi[21], J. I. Rawlings[30], G. Raymond[9], D. Rigopoulou[31,33], L. Riguccini[6], D. Rizzo[10], G. Rodighiero[20], I. G. Roseboom[19], M. Rowan-Robinson[10], A. Saintonge[3], M. Sanchez Portal[7], P. Santini[17], B. Schulz[11,24], D. Scott[22], N. Seymour[30], L. Shao[3], D. L. Shupe[11,24], A. J. Smith[19], J. A. Stevens[34], E. Sturm[3], M. Symeonidis[30], L. Tacconi[3], M. Trichas[10], K. E. Tugwell[30], M. Vaccari[20], I. Valtchanov[7], J. Vieira[11], L. Vigroux[28], L. Wang[19], R. Ward[19], G. Wright[1], C. K. Xu[11,24], and M. Zemcov[11,12]

(Affiliations are available in the online edition)

Received 30 March 2010 / Accepted 23 April 2010

ABSTRACT

We set out to determine the ratio, $q_{\rm IR}$, of rest-frame 8–1000-μm flux, $S_{\rm IR}$, to monochromatic radio flux, $S_{\rm 1.4\,GHz}$, for galaxies selected at far-infrared (IR) and radio wavelengths, to search for signs that the ratio evolves with redshift, luminosity or dust temperature, $T_{\rm d}$, and to identify any far-IR-bright outliers – useful laboratories for exploring why the far-IR/radio correlation (FIRRC) is generally so tight when the prevailing theory suggests variations are almost inevitable. We use flux-limited 250-μm and 1.4-GHz samples, obtained using *Herschel* and the Very Large Array (VLA) in GOODS-North (-N). We determine bolometric IR output using ten bands spanning $\lambda_{\rm obs} = 24{-}1250\,\mu$m, exploiting data from PACS and SPIRE (PEP; HerMES), as well as *Spitzer*, SCUBA, AzTEC and MAMBO. We also explore the properties of an $L_{\rm IR}$-matched sample, designed to reveal evolution of $q_{\rm IR}$ with redshift, spanning log $L_{\rm IR} = 11$–$12\,L_\odot$ and $z = 0$–2, by stacking into the radio and far-IR images. For 1.4-GHz-selected galaxies in GOODS-N, we see tentative evidence of a break in the flux ratio, $q_{\rm IR}$, at $L_{\rm 1.4\,GHz} \sim 10^{22.7}$ W Hz^{-1}, where active galactic nuclei (AGN) are starting to dominate the radio power density, and of weaker correlations with redshift and $T_{\rm d}$. From our 250-μm-selected sample we identify a small number of far-IR-bright outliers, and see trends of $q_{\rm IR}$ with $L_{\rm 1.4\,GHz}$, $L_{\rm IR}$, $T_{\rm d}$ and redshift, noting that some of these are inter-related. For our $L_{\rm IR}$-matched sample, there is no evidence that $q_{\rm IR}$ changes significantly as we move back into the epoch of galaxy formation: we find $q_{\rm IR} \propto (1+z)^\gamma$, where $\gamma = -0.04 \pm 0.03$ at $z = 0-2$; however, discounting the least reliable data at $z < 0.5$ we find $\gamma = -0.26 \pm 0.07$, modest evolution which may be related to the radio background seen by ARCADE 2, perhaps driven by <10-μJy radio activity amongst ordinary star-forming galaxies at $z > 1$.

Key words. galaxies: evolution – galaxies: starburst – infrared: galaxies – submillimeter: galaxies – radio continuum: galaxies

1. Introduction

For samples of local galaxies – on galactic and ~100-pc scales – there is a good correlation between far-IR and radio emission (de Jong et al. 1985; Helou et al. 1985; Condon et al. 1991; Yun et al. 2001). The correlation spans many orders of magnitude in luminosity, gas surface density and photon, cosmic-ray and magnetic energy density, and arises because the far-IR and radio wavelength regimes share a common link with luminous, massive stars and their end products – dust, supernovae (SNe) and cosmic rays. In the simplest models (dubbed "calorimetry" – e.g. Voelk 1989; Lisenfeld et al. 1996), dust absorbs all of the ultraviolet radiation from massive stars, re-radiating this energy in the far-IR, and when those massive stars explode as SNe they generate cosmic-ray electrons which lose all their energy in the radio regime, mainly via synchrotron emission. A balance is thereby achieved between far-IR and radio emission, assuming that the starburst timescale is sufficiently long (>10^7 yr).

Traditionally, $L_{\rm IR}$ and $L_{\rm radio}$ are both employed to determine star-formation rates, and the far-IR/radio flux density ratio has been useful when estimating the redshift or $T_{\rm d}$ of a distant starburst, or when defining samples of AGN (Condon 1992; Carilli & Yun 1999; Ivison et al. 2002; Bell 2003; Chapman et al. 2005; Donley et al. 2005), or probing magnetic field strength (Thompson et al. 2006). For these reasons, and because of recent observational advances at both far-IR and radio wavelengths, there has been a deluge of FIRRC-related work

★ *Herschel* is an ESA space observatory with science instruments provided by European-led Principal Investigator consortia and with important participation from NASA.

recently, exploring why the correlation exists and whether it continues to hold at progressively larger look-back times (Garrett 2002; Appleton et al. 2004; Ibar et al. 2008; Seymour et al. 2009; Ivison et al. 2010; Sargent et al. 2010a). Prevailing theory (e.g. Lacki et al. 2010) suggests that variations in the far-IR/radio flux ratio should be virtually unavoidable and that the FIRRC thus arises due to a mysterious combination of effects involving bremsstrahlung, inverse Compton cooling, ionisation and the relative fractions of primary/secondary cosmic-ray electrons/protons, as well as the critical synchrotron frequency.

Aside from the modelling work of Lacki et al., recent advances in this field have included the use of luminosity-matched samples (between high and low redshift) to better probe evolution with look-back time (Sargent et al. 2010b) and the use of measurements spanning the far-IR and radio wavebands to avoid assumptions relating to k corrections (Ivison et al. 2010), although Calzetti et al. (2010) have argued that bands beyond 24 μm contain a contribution from dust heated by stars from previous episodes of star formation and so we might not necessarily expect the correlation to improve. In this paper we introduce flux-limited 250-μm- and 1.4-GHz-selected samples of galaxies from *Herschel* and the VLA, as well as a luminosity-matched sample selected at 24 μm, spanning $z = 0$–2, and determine their spectral energy distributions (SEDs) spanning the entire far-IR spectral region. We then investigate the FIRRC from the perspectives of the 24-, 250-μm- and radio-selected samples.

2. Sample selection and data analysis

In this paper we present results from observations with *Herschel* (Pilbratt et al. 2010). The SPIRE instrument, its in-orbit performance, and its scientific capabilities are described by Griffin et al. (2010), and the SPIRE astronomical calibration methods and accuracy are outlined in Swinyard et al. (2010). PACS is described by Poglitsch et al. (2010).

Our datasets are drawn from the common area observed by PACS and SPIRE at 100, 160, 250, 350 and 500 μm as part of HerMES[1] (Oliver et al., in prep.) and PEP (Lutz et al., in prep.) in the GOODS-N field, prior to acquisition of data for GOODS-*Herschel*. GOODS-N has also been observed with the VLA at 1.4 GHz (1.7″ *FWHM* – Biggs & Ivison 2006; Morrison et al. 2010) and *Spitzer* at 24, 70 and 160 μm; we make use of these data, as well as the 850-, 1100- and 1250-μm images of Borys et al. (2003), Perera et al. (2008) and Greve et al. (2008).

We employ three GOODS-N galaxy samples, all selected above a signal-to-noise threshold of 5σ:

1. 128 galaxies selected at 250 μm, without priors, with $S_{250\,\mu\mathrm{m}} \gtrsim 20$ mJy (Fig. 1; Smith et al., in prep.);
2. 247 galaxies selected at 1.4 GHz (Fig. 1) with a $S_{1.4\,\mathrm{GHz}}$ limit of $\sim$20 μJy, 137 with spectroscopic redshifts (Barger et al. 2008), the remainder with photometric redshifts ($\langle z \rangle = 0.94$; interquartile z, 0.56–1.76);
3. a L_{IR}-matched sample of 652 sources spanning $z = 0$–2, selected initially at 24 μm (Magnelli et al. 2009; Berta et al. 2010) then filtered to cover only the decade of L_{IR} between $10^{11} \rightarrow 10^{12}\ L_{\odot}$ (LIRGs), where L_{IR} is determined using the models of Chary & Elbaz (2001).

Far-IR and submm flux densities for the three samples are determined using images convolved with appropriate point spread functions. S_{IR} is calculated by integrating under the well-sampled SEDs. Monte-Carlo simulations are used to assess the uncertainty in S_{IR}. The formal error on $S_{24\,\mu\mathrm{m}}$ was boosted by 3× to account for the uncertain shape of the SED between rest-frame 8–70 μm. A modified blackbody fit to the measurements beyond 24 μm (with the emissivity index, $\beta = 1.5$) was used to determine T_{d}.

For sample (1), additional procedures are implemented to define a clean sample, free from blends: following the procedure of Downes et al. (1986), 107/128 sources are found to have secure ($P < 0.05$) radio identifications (ids) within a search radius, $r = 10''$; we discard the remainder. To avoid using those sources most severely affected by blending, we further discard those with more than one radio emitter within r, leaving 65 sources. Of the galaxies without a secure radio id, three have no plausible radio ids within r: a potentially interesting sub-sample. Measurements are made at the radio positions for the 65 sources with secure, unambiguous ids, and at the 250-μm positions for the three sources without radio emission.

For sample (2), far-IR and submm measurements are made at the radio positions.

For the L_{IR}-matched galaxies (sample 3), median stacking is used to measure S_{IR} and $S_{1.4\,\mathrm{GHz}}$: we follow the procedure outlined by Ivison et al. (2010). Fluxes are calculated from 31^2-pixel^2 stacked images in the ten available filters and S_{IR} is determined as before.

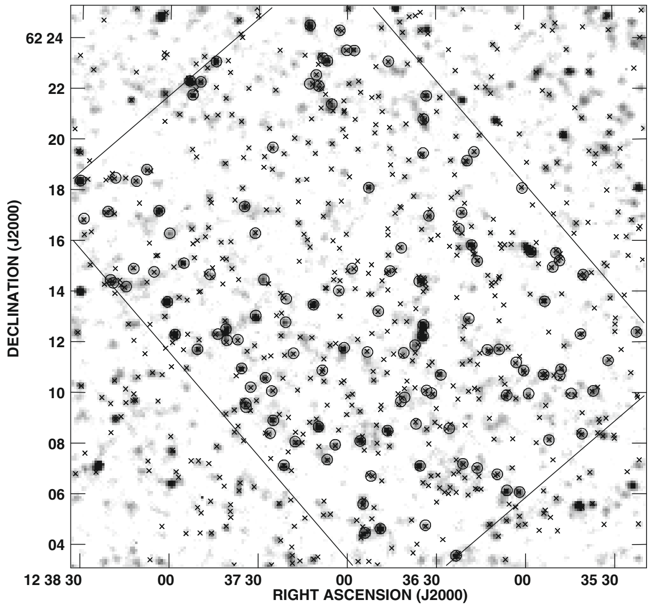

Fig. 1. 250-μm image of GOODS-N, with $\geq$5-σ 250-μm [radio] sources marked by circles [crosses]. The PACS region is also indicated. Here, σ includes instrumental and confusion noise combined in quadrature, where $\sigma_{\mathrm{conf}}/\sigma_{\mathrm{instr}} \sim 5$ (cf. $\sim$2 for BLAST).

3. Results and conclusions

q_{IR} as utilised here is the logarithmic ratio of the rest-frame 8–1000-μm flux, S_{IR}, and the 1.4-GHz flux density, $S_{1.4\,\mathrm{GHz}}$, such that $q_{\mathrm{IR}} = \log_{10}\ [(S_{\mathrm{IR}}/3.75 \times 10^{12}\ \mathrm{W\,m^{-2}})/(S_{1.4\,\mathrm{GHz}}/\mathrm{W\ m^{-2}\ Hz^{-1}})]$, where $S_{1.4\,\mathrm{GHz}}$ is k-corrected assuming $S_{\nu} \propto \nu^{\alpha}$, with $\alpha = -0.8$.

We begin with sample (1), those selected at 250 μm: q_{IR} is not a strong function of S_{IR} (Fig. 2), nor of $S_{1.4\,\mathrm{GHz}}$. We see no evidence of contamination by radio-loud AGN, consistent with

[1] hermes.sussex.ac.uk

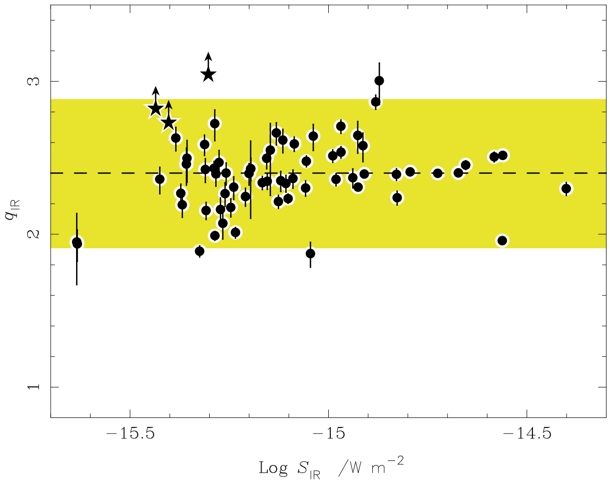

Fig. 2. $q_{\rm IR}$ versus $S_{\rm IR}$ for those 250-μm-selected galaxies (sample 1) with secure, unambiguous radio ids. Those without plausible radio ids are plotted as stars. The dashed line is the median, $q_{\rm IR} = 2.40$; the shaded region represents $\pm 2\sigma_q$ ($\sigma_q = 0.24$).

Table 1. Trends.

$q_{\rm IR}$ trend	Spear-man ρ	Signifi-cance
Sample 1 (250-μm-selected galaxies with redshifts):		
(5.02 ± 0.18)–$(0.105 \pm 0.008) \log L_{1.4\,\rm GHz}$	−0.48	99.8%
(6.09 ± 0.33)–$(0.092 \pm 0.008) \log L_{\rm IR}$	−0.32	95.6%
(2.61 ± 0.02)–$(0.081 \pm 0.007)\,(1{+}z)$	−0.33	96.0%
(2.76 ± 0.03)–$(0.008 \pm 0.001)\,T_{\rm d}$	−0.33	96.1%
Sample 2 (radio-selected galaxies with redshifts):		
(4.92 ± 0.21)–$(0.101 \pm 0.009) \log L_{1.4\,\rm GHz}$	−0.27	99.9%
(2.74 ± 0.35)–$(0.007 \pm 0.009) \log L_{\rm IR}$	+0.07	69.1%
(2.55 ± 0.02)–$(0.047 \pm 0.010)\,(1{+}z)$	−0.15	96.6%
(2.60 ± 0.02)–$(0.002 \pm 0.001)\,T_{\rm d}$	−0.16	89.2%

the findings of Yun et al. (2001). Some galaxies stand out as potentially far-IR-bright: these include the three galaxies without plausible radio ids, two of which are detected at 70 and/or 160 μm, so are likely at low redshift with their radio emission resolved away.

Only 39/65 sources with unambiguous radio ids have redshifts (20 photometric, 19 spectroscopic; $\langle z \rangle = 0.98$; interquartile $z = 0.46$–1.52, similar to sample 2). Nevertheless, this sub-sample allows us to explore correlations between $q_{\rm IR}$ and luminosity, redshift and $T_{\rm d}$. We find significant (>95% confidence – Table 1) trends for lower $q_{\rm IR}$ amongst the most radio- and far-IR-luminous galaxies, and the warmest and most distant, though these parameters are likely inter-related. The dependence of $q_{\rm IR}$ on $L_{1.4\,\rm GHz}$ is the strongest and likely reflects the influence of low-radio-power AGN, of which more later; that of $q_{\rm IR}$ on $L_{\rm IR}$ is more puzzling, perhaps reflecting the dependence of $L_{\rm IR}$ on redshift and/or $T_{\rm d}$ (e.g. Chapman et al. 2005), or selection effects (since this trend is not seen for sample 2 – see Table 1).

Figure 3 shows $q_{\rm IR}$ versus redshift for our radio-selected galaxies (sample 2), split into five log-spaced bins of $L_{1.4\,\rm GHz}$. Does $q_{\rm IR}$ evolve with redshift? One might conclude that it does, based on the bottom panel of Fig. 3, where $q_{\rm IR} \propto (1+z)^{\gamma}$, with $\gamma = -0.05 \pm 0.01$ (Table 1). However, we must be aware of some strong selection effects which make this evidence unreliable: radio emission can be due to an AGN and several radio-loud objects with low values of $q_{\rm IR}$ are obvious in Fig. 3. Such AGN are more common at $z \sim 2$ than today (e.g. Wall et al. 2005); moreover, radio emission from faint starbursts (with $\alpha = -0.8$, although see Ibar et al. 2010) becomes

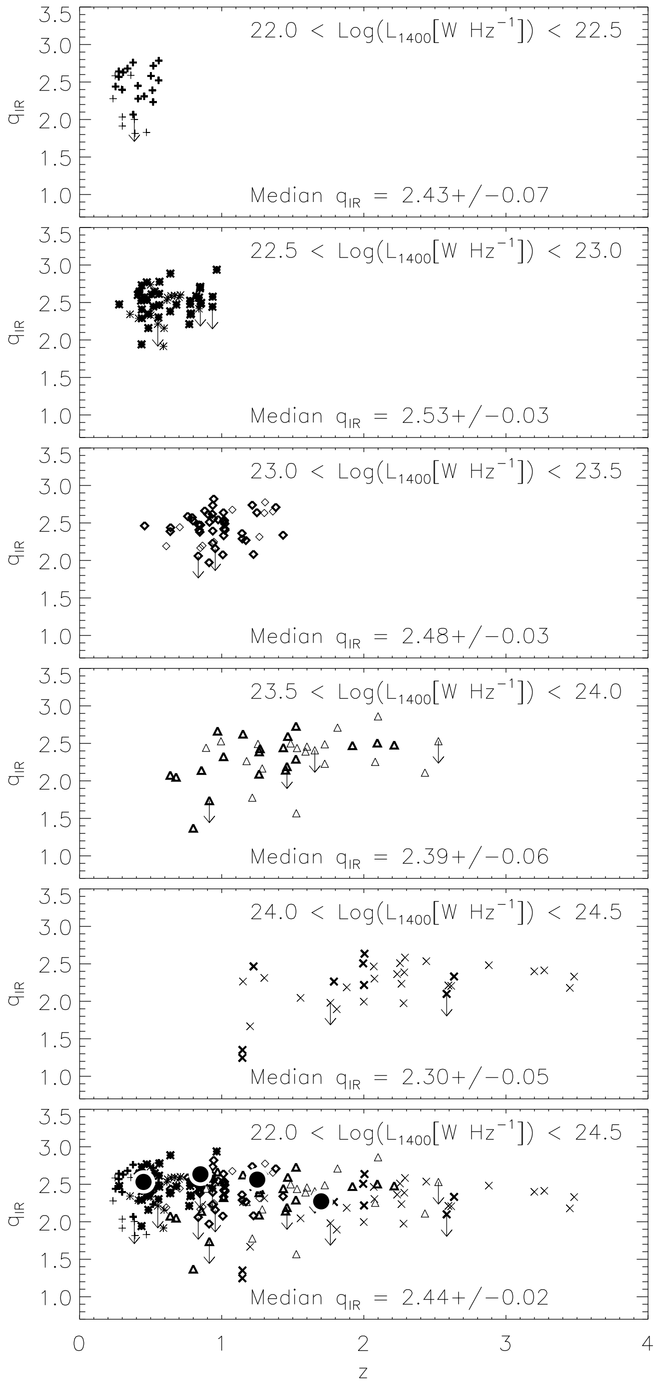

Fig. 3. $q_{\rm IR}$ versus redshift for our radio-selected galaxies (sample 2), in five bins of K-corrected $L_{1.4\,\rm GHz}$, plus the full sample. Values of $q_{\rm IR}$ for sample 3 are shown (as circles) for comparison.

more difficult to detect at higher redshifts, such that the fraction of radio-loud AGN in a flux-limited sample will rise, driving down $q_{\rm IR}$. Indeed, Fig. 4 shows tentative evidence of a break in $\langle q_{\rm IR} \rangle$ at $L_{1.4\,\rm GHz} \sim 10^{22.7}$ W Hz^{-1}. One might also expect radio-loud objects (those with low $q_{\rm IR}$) to contain warmer, AGN-heated dust, giving rise to the weak trend (89.2% confidence – Table 1) of decreasing $q_{\rm IR}$ with increasing $T_{\rm d}$.

Finally, we turn to our $L_{\rm IR}$-matched galaxies (sample 3), illustrated in Fig. 5. The $\delta z = 0.5$ bins provide significant numbers of objects at near-constant $L_{\rm IR}$ spanning $z = 0$–2. As well as being matched in $L_{\rm IR}$, there is another key difference between our new sample and that used by Ivison et al. (2010): although

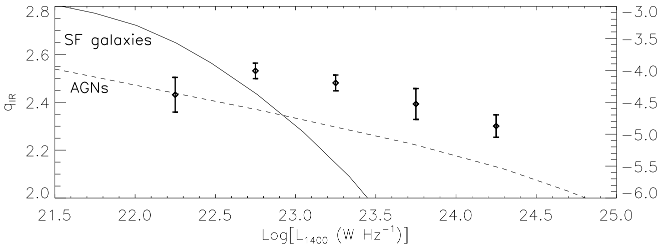

Fig. 4. Median q_{IR} versus $L_{1.4\,GHz}$. The local luminosity functions of starbursts and AGN are shown (Mauch & Sadler 2007).

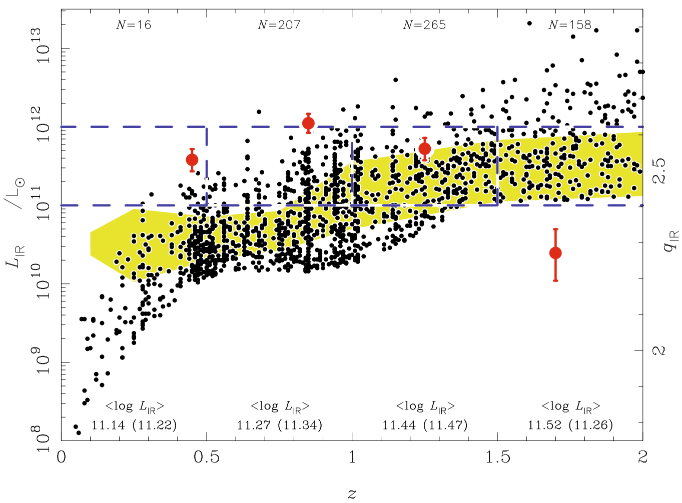

Fig. 5. L_{IR} (dots; left axis) and q_{IR} (red circles; right axis) – the former determined via the models of Chary & Elbaz (2001) – versus redshift for our L_{IR}-matched sample. The luminosity bounds and redshift bins (dashed lines), the number of galaxies in each bin and their predicted (measured) $\langle \log L_{IR} \rangle$ and measured $\langle q_{IR} \rangle$ are all shown. The shaded area represents a $\pm 1\sigma$ prediction for q_{IR} (Swinbank et al. 2008; Ivison et al. 2010).

the new sample is based initially on a flux-limited 24-μm catalogue, the final selection is based on L_{IR}, with model-dependent extrapolations from the mid-IR (accurate to $\lesssim 2\times$ across all bins – Fig. 5). This should lead to less contamination by AGN at the blue end of the rest-frame 8–1000-μm band, where the relative contribution to S_{IR} can be substantial (Fig. 11 – Ivison et al. 2010). Using our new sample, there is no strong evidence that q_{IR} changes as we move back into the epoch of galaxy formation at $z \sim 2$, with $\gamma = -0.04 \pm 0.03$ where $q_{IR} \propto (1+z)^\gamma$, consistent with the findings of Sargent et al. (2010b). If we discount the $z < 0.5$ data, which comprise only 16 galaxies which are not well matched in L_{IR} to the higher redshift bins, we find $\gamma = -0.26 \pm 0.07$. This is similar to the $\gamma = -0.15 \pm 0.03$ found by Ivison et al. (2010) who noted reports that evolution in q_{IR} could be related to the radio background seen by ARCADE 2 (Fixsen et al. 2009; Seiffert et al. 2010). Our sample, with $\langle S_{1.4\,GHz} \rangle \lesssim 10\,\mu$Jy at $z \gtrsim 1$, is consistent with the idea that evolution of the FIRRC might be driven by <10-μJy radio activity amongst ordinary star-forming galaxies at $z > 1$ (Singal et al. 2010).

Acknowledgements. The data presented in this paper will be released through the *Herschel* Database in Marseille HeDaM (`hedam.oamp.fr/HerMES`). SPIRE has been developed by a consortium of institutes led by Cardiff Univ. (UK) and including Univ. Lethbridge (Canada); NAOC (China); CEA, LAM (France); IFSI, Univ. Padua (Italy); IAC (Spain); Stockholm Observatory (Sweden); Imperial College London, RAL, UCL-MSSL, UKATC, Univ. Sussex (UK); Caltech, JPL, NHSC, Univ. Colorado (USA). This development has been supported by national funding agencies: CSA (Canada); NAOC (China); CEA, CNES, CNRS (France); ASI (Italy); MCINN (Spain); SNSB (Sweden); STFC (UK); and NASA (USA). PACS has been developed by a consortium of institutes led by MPE (Germany) and including UVIE (Austria); KUL, CSL, IMEC (Belgium); CEA, OAMP (France); MPIA (Germany); IFSI, OAP/AOT, OAA/CAISMI, LENS, SISSA (Italy); IAC (Spain). This development has been supported by the funding agencies BMVIT (Austria), ESA-PRODEX (Belgium), CEA/CNES (France), DLR (Germany), ASI (Italy), and CICYT/MCYT (Spain).

References

Appleton, P. N., Fadda, D., Marleau, F., et al. 2004, ApJS, 154, 147
Barger, A. J., Cowie, L. L., & Wang, W. 2008, ApJ, 689, 687
Bell, E. F. 2003, ApJ, 586, 794
Berta, S., Magnelli, B., Lutz, D., et al. 2010, A&A, 518, L30
Biggs, A. D., & Ivison, R. J. 2006, MNRAS, 371, 963
Borys, C., Chapman, S., Halpern, M., & Scott, D. 2003, MNRAS, 344, 385
Calzetti, D., Wu, S., Hong, S., et al. 2010, ApJ, 714, 1256
Carilli, C. L., & Yun, M. S. 1999, ApJ, 513, L13
Chapman, S. C., Blain, A., Smail, I., & Ivison, R. 2005, ApJ, 622, 772
Chary, R., & Elbaz, D. 2001, ApJ, 556, 562
Condon, J. J. 1992, ARA&A, 30, 575
Condon, J. J., Anderson, M. L., & Helou, G. 1991, ApJ, 376, 95
de Jong, T., Klein, U., Wielebinski, R., & Wunderlich, E. 1985, A&A, 147, L6
Donley, J., Rieke, G., Rigby, J., & Pérez-González, P. 2005, ApJ, 634, 169
Downes, A. J. B., Peacock, J. A., Savage, A., & Carrie, D. R. 1986, MNRAS, 218, 31
Fixsen, D. J., Kogut, A., Levin, S., et al. 2009, ApJ, submitted [`arXiv:0901.0555`]
Garrett, M. A. 2002, A&A, 384, L19
Greve, T. R., Pope, A., Scott, D., et al. 2008, MNRAS, 389, 1489
Griffin, M. J., Abergel, A., Abreu, A., et al. 2010, A&A, 518, L3
Helou, G., Soifer, B. T., & Rowan-Robinson, M. 1985, ApJ, 298, L7
Ibar, E., Cirasuolo, M., Ivison, R., et al. 2008, MNRAS, 386, 953
Ibar, E., Ivison, R. J., Best, P. N., et al. 2010, MNRAS, 401, L53
Ivison, R. J., Alexander, D., Biggs, A., et al. 2010, MNRAS, 402, 245
Ivison, R. J., Greve, T. R., Smail, I., et al. 2002, MNRAS, 337, 1
Lacki, B. C., Thompson, T. A., & Quataert, E. 2010, ApJ, 717, 1
Lisenfeld, U., Voelk, H. J., & Xu, C. 1996, A&A, 314, 745
Magnelli, B., Elbaz, D., Chary, R. R., et al. 2009, A&A, 496, 57
Mauch, T., & Sadler, E. M. 2007, MNRAS, 375, 931
Morrison, G. E., Owen, F. N., Dickinson, M. E., Ivison, R. J., & Ibar, E. 2010, ApJS, 188, 178
Perera, T., Chapin, E., Austermann, J., et al. 2008, MNRAS, 391, 1227
Pilbratt, G. L., et al. 2010, A&A, 518, L1
Poglitsch, A. et al. 2010, A&A, 518, L2
Sargent, M., Schinnerer, E., Murphy, E., et al. 2010a, ApJS, 186, 341
Sargent, M., Schinnerer, E., Murphy, E., et al. 2010b, ApJ, 714, L190
Seiffert, M., Fixsen, D. J., Kogut, A., et al. 2010, [`arXiv:0901.0559`]
Seymour, N., Huynh, M., Dwelly, T., et al. 2009, MNRAS, 398, 1573
Singal, J., Stawarz, L., Lawrence, A., & Petrosian, V. 2010, MNRAS, submitted [`arXiv:0909.1997`]
Swinbank, A. M., Lacey, C., Smail, I., et al. 2008, MNRAS, 391, 420
Swinyard, B. M., Ade, P., Baluteau, J.-P., et al. 2010, A&A, 518, L4
Thompson, T. A., Quataert, E., Waxman, E., Murray, N., & Martin, C. L. 2006, ApJ, 645, 186
Voelk, H. J. 1989, A&A, 218, 67
Wall, J. V., Jackson, C. A., Shaver, P. A., Hook, I. M., & Kellermann, K. I. 2005, A&A, 434, 133
Yun, M. S., Reddy, N. A., & Condon, J. J. 2001, ApJ, 554, 803

Page 5 is available in the electronic edition of the journal at `http://www.aanda.org`

[1] UK Astronomy Technology Centre, Royal Observatory, Blackford Hill, Edinburgh EH9 3HJ, UK
e-mail: rji@roe.ac.uk
[2] Institute for Astronomy, University of Edinburgh, Royal Observatory, Blackford Hill, Edinburgh EH9 3HJ, UK
[3] Max-Planck-Institut für Extraterrestrische Physik (MPE), Postfach 1312, 85741, Garching, Germany
[4] ESO, Karl-Schwarzschild-Str. 2, 85748 Garching bei München, Germany
[5] INAF - Osservatorio Astronomico di Trieste, via Tiepolo 11, 34143 Trieste, Italy
[6] Laboratoire AIM-Paris-Saclay, CEA/DSM/Irfu – CNRS – Université Paris Diderot, CE-Saclay, pt courrier 131, 91191 Gif-sur-Yvette, France
[7] *Herschel* Science Centre, European Space Astronomy Centre, Villanueva de la Cañada, 28691 Madrid, Spain
[8] Department of Physics & Astronomy, University of California, Irvine, CA 92697, USA
[9] Cardiff School of Physics and Astronomy, Cardiff University, Queens Buildings, The Parade, Cardiff CF24 3AA, UK
[10] Astrophysics Group, Imperial College London, Blackett Laboratory, Prince Consort Road, London SW7 2AZ, UK
[11] California Institute of Technology, 1200 E. California Blvd, Pasadena, CA 91125, USA
[12] Jet Propulsion Laboratory, 4800 Oak Grove Drive, Pasadena, CA 91109, USA
[13] Instituto de Astrofísica de Canarias (IAC) and Departamento de Astrofísica, Universidad de La Laguna (ULL), La Laguna, Tenerife, Spain
[14] Laboratoire d'Astrophysique de Marseille, OAMP, Université Aix-marseille, CNRS, 38 rue Frédéric Joliot-Curie, 13388 Marseille cedex 13, France
[15] Dipartimento di Astronomia, Università di Bologna, Via Ranzani 1, 40127 Bologna, Italy
[16] Department of Astrophysical and Planetary Sciences, CASA 389-UCB, University of Colorado, Boulder, CO 80309, USA
[17] INAF - Osservatorio Astronomico di Bologna, via Ranzani 1, I-40127 Bologna, Italy
[18] Observational Cosmology Laboratory, Code 665, NASA Goddard Space Flight Center, Greenbelt, MD 20771, USA
[19] Astronomy Centre, Department of Physics & Astronomy, University of Sussex, Brighton BN1 9QH, UK
[20] Dipartimento di Astronomia, Università di Padova, vicolo Osservatorio, 3, 35122 Padova, Italy
[21] INAF - Osservatorio Astronomico di Roma, via di Franscati 33, 00040 Monte Porzio Catone, Italy
[22] Department of Physics and Astronomy, University of British Columbia, 6224 Agricultural Road, Vancouver, BC V6T 1Z1, Canada
[23] Institut d'Astrophysique Spatiale (IAS), bâtiment 121, Université Paris-Sud 11 and CNRS (UMR 8617), 91405 Orsay, France
[24] Infrared Processing and Analysis Center, MS 100-22, California Institute of Technology, JPL, Pasadena, CA 91125, USA
[25] School of Physics and Astronomy, The University of Manchester, Alan Turing Building, Oxford Road, Manchester M13 9PL, UK
[26] Institute for Astronomy, University of Hawaii, Honolulu, HI 96822, USA
[27] Canada-France-Hawaii Telescope, Kamuela, HI, 96743, USA
[28] Institut d'Astrophysique de Paris, UMR 7095, CNRS, UPMC Univ. Paris 06, 98bis boulevard Arago, 75014 Paris, France
[29] National Radio Astronomy Observatory, PO Box O, Socorro NM 87801, USA
[30] Mullard Space Science Laboratory, University College London, Holmbury St. Mary, Dorking, Surrey RH5 6NT, UK
[31] Space Science and Technology Department, Rutherford Appleton Laboratory, Chilton, Didcot, Oxfordshire OX11 0QX, UK
[32] Institute for Space Imaging Science, University of Lethbridge, Lethbridge, Alberta T1K 3M4, Canada
[33] Astrophysics, Oxford University, Keble Road, Oxford OX1 3RH, UK
[34] Centre for Astrophysics Research, University of Hertfordshire, College Lane, Hatfield, Hertfordshire AL10 9AB, UK